Supporting Information for

Effective accommodation and conversion of polysulfide using organic-inorganic hybrid frameworks for long-life lithium-sulfur battery

Sa Jiao, Tianyi Ding, Rui Zhai, Yunping Wu, Sheng Chen, and Wei Wei*

Department of Applied Chemistry, School of Science, MOE Key Laboratory for Nonequilibrium Synthesis and Modulation of Condensed Materials, Xi'an Key Laboratory of Sustainable Energy Material Chemistry, Xi'an Jiaotong University, Xi'an 710049, P R China.
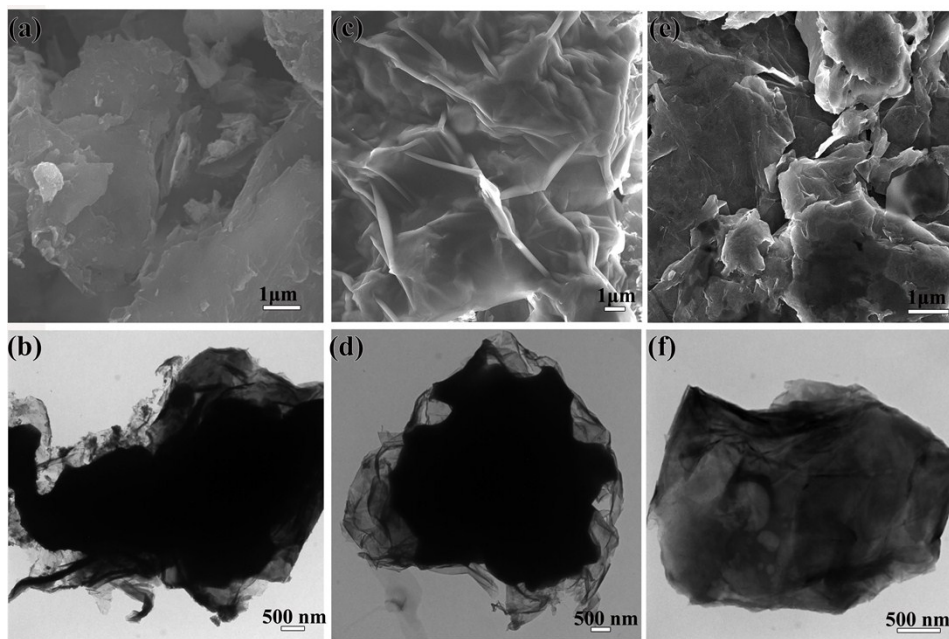
*E-mail: wwei.mc@mail.xjtu.edu.cn

Figure S1. (a) SEM and (b) TEM images of Co_3O_4@G-S; (c) SEM and (d) TEM images of G-S; (e) SEM and (f) TEM images of RCE@G-S.
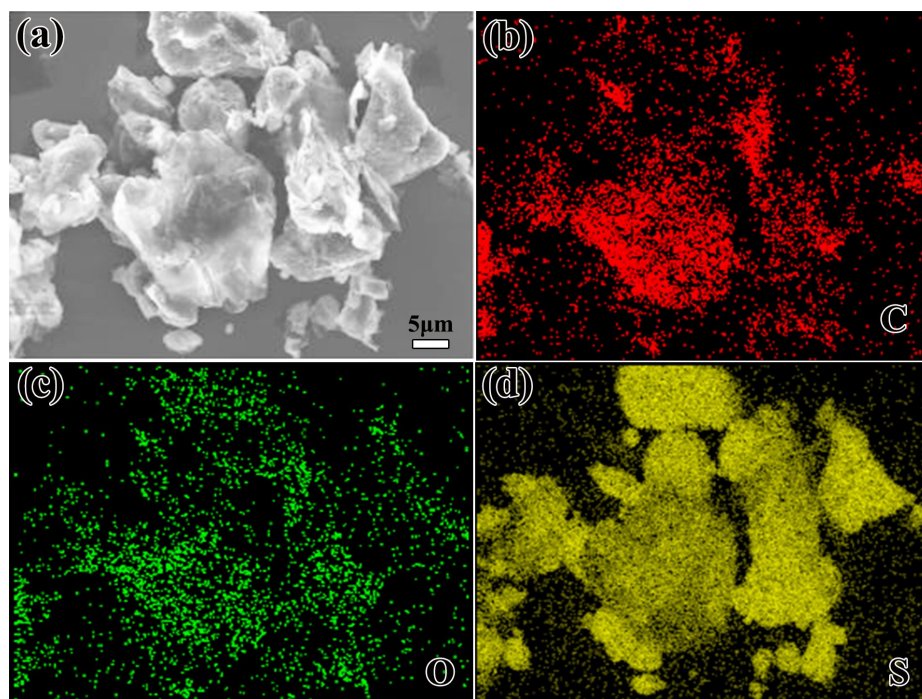

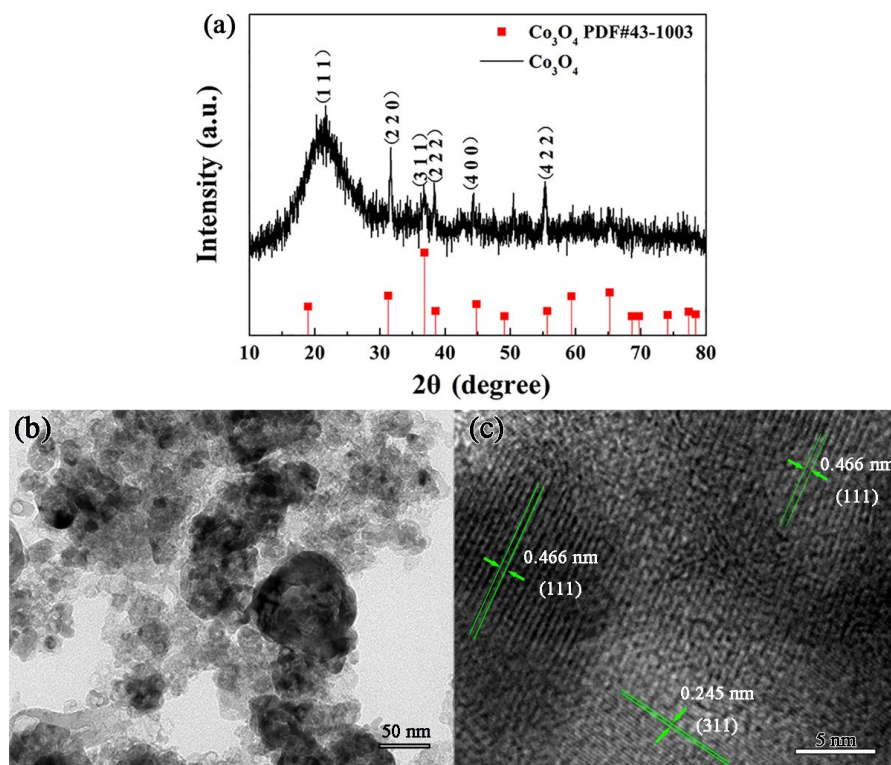**Figure S2**. (a) SEM and (b-d) EDX mapping images for C, O, S elements of RCE@G-S composite.

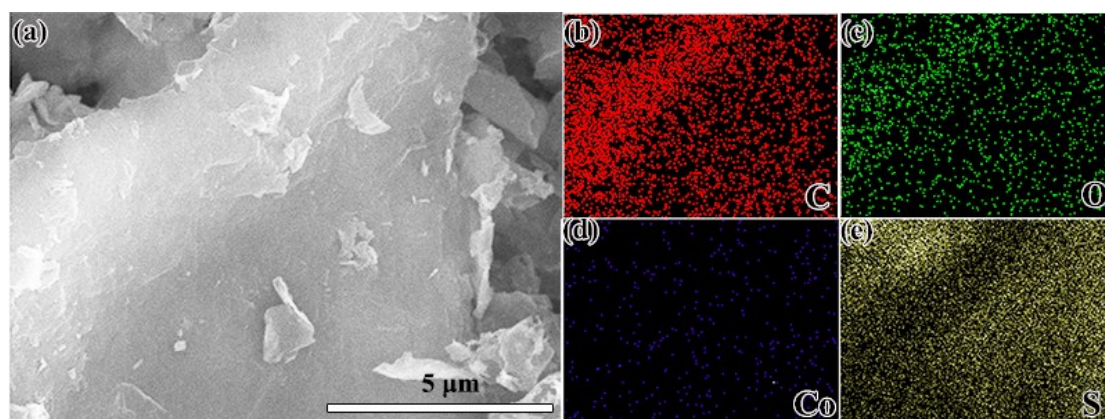**Figure S3**. (a) XRD pattern, (b) TEM and (c) HRTEM images of Co$_3$O$_4$ NCs.

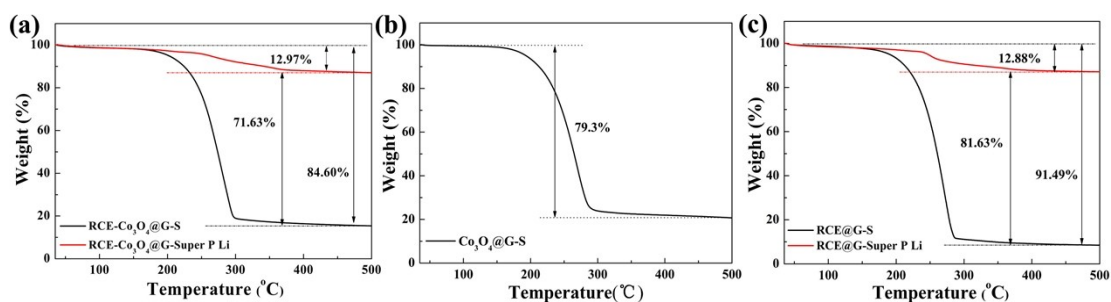**Figure S4**. EDX mapping for (a) SEM image, (b) C, (c) O, (d) Co, and (e) S of Co$_3$O$_4$@G-S composite.

Figure S5. TGA of the RCE-Co$_3$O$_4$@G-S (a), Co$_3$O$_4$@G-S (b), RCE@G-S (c).

Among the range of 35-500 °C in N$_2$ atmosphere, both S and CE underwent thermal decomposition with weight loss. Accordingly, we needed to exclude the influence of CE by replacing the sulfur of RCE-Co$_3$O$_4$@G-S with same amount of Super P Li for TGA measurement. Therefore, by calculating the difference (subtraction) between the thermal decomposition loss of RCE-Co$_3$O$_4$@G-S and RCE-Co$_3$O$_4$@G-Super P Li, the sulfur content in RCE-Co$_3$O$_4$@G-S could be obtained (71.63%). The sulfur content in RCE@G-S was calculated by the same method (81.63%).
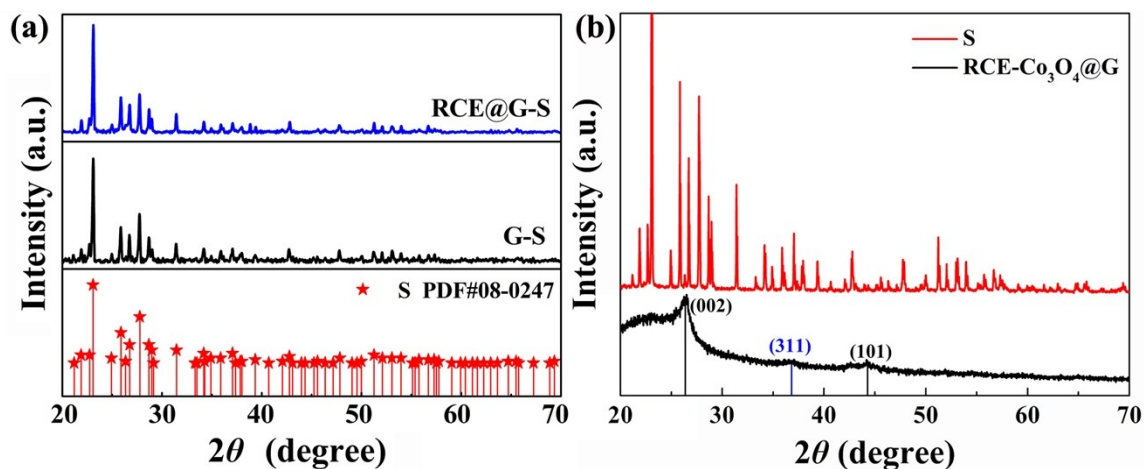

Figure S6. (a) XRD patterns of RCE@G-S and G-S composites; (b) XRD patterns of RCE-Co$_3$O$_4$@G matrix and pristine sulfur. For RCE-Co$_3$O$_4$@G, the diffraction peaks from graphene and Co$_3$O$_4$ are marked in black and blue color respectively.
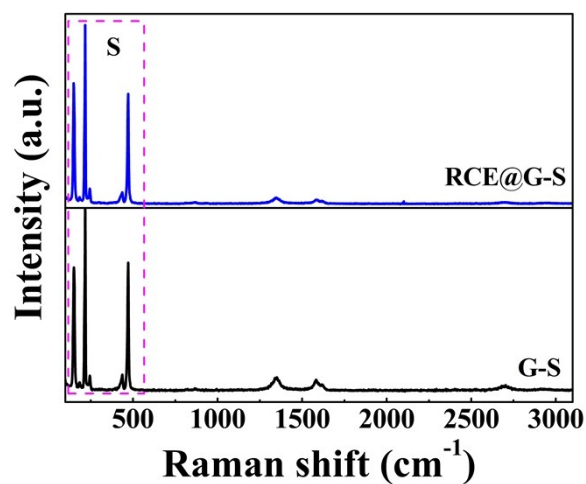
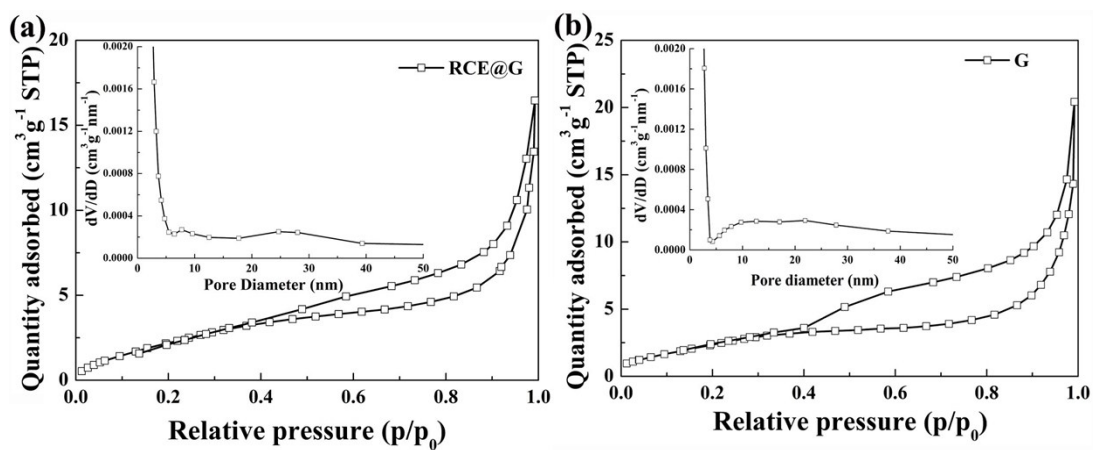Figure S7. Raman spectra of RCE@G-S and G-S composites.

Figure S8. N_2 adsorption-desorption isotherms and pore size distribution (inset) of RCE@G (a) and G (b) respectively.

Table S1. RCE-Co$_3$O$_4$@G-S surface element content based on XPS.

Element	C1s	O1s	Co2p	S2p	N1s
Atom %	75.48	18.65	1.07	2.37	2.48

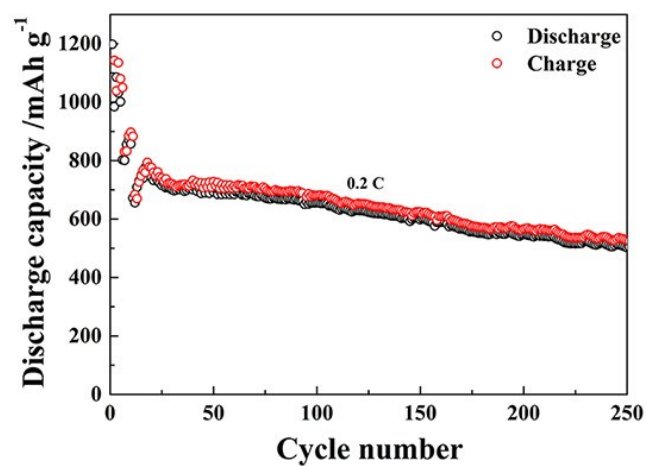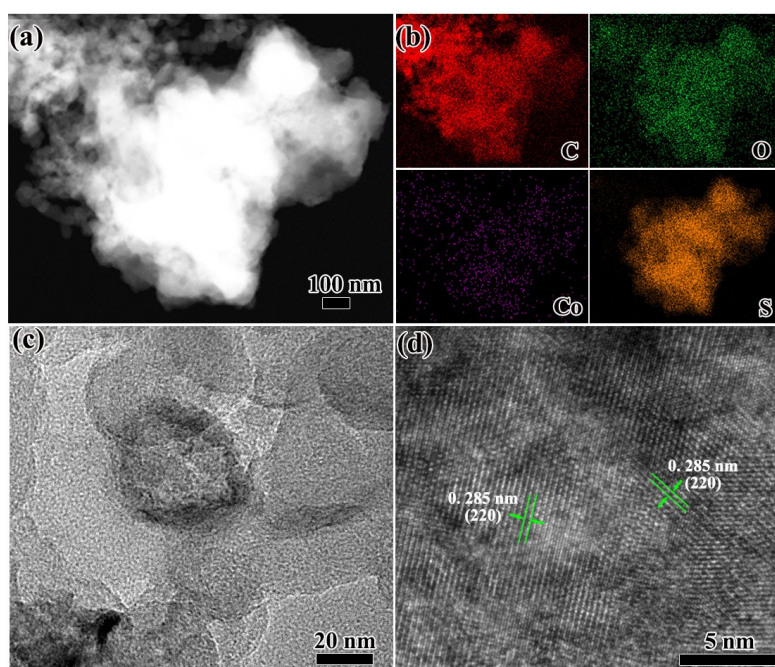**Figure S9.** Cycling performance of RCE-Co$_3$O$_4$@G-S with sulfur loading of 1.6 mg cm^{-2}.

Figure S10. (a, b) STEM image and corresponding elemental mapping images of RCE-Co$_3$O$_4$@G-S cathode after 100 cycles. (c, d) HR-TEM images of incorporated Co$_3$O$_4$.
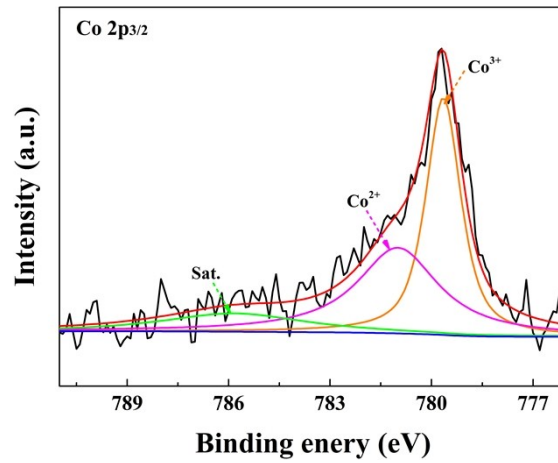
Figure S11. High-resolution Co 2p$_{3/2}$ XPS spectra of RCE-Co$_3$O$_4$@G-S cathode after 100 cycles.
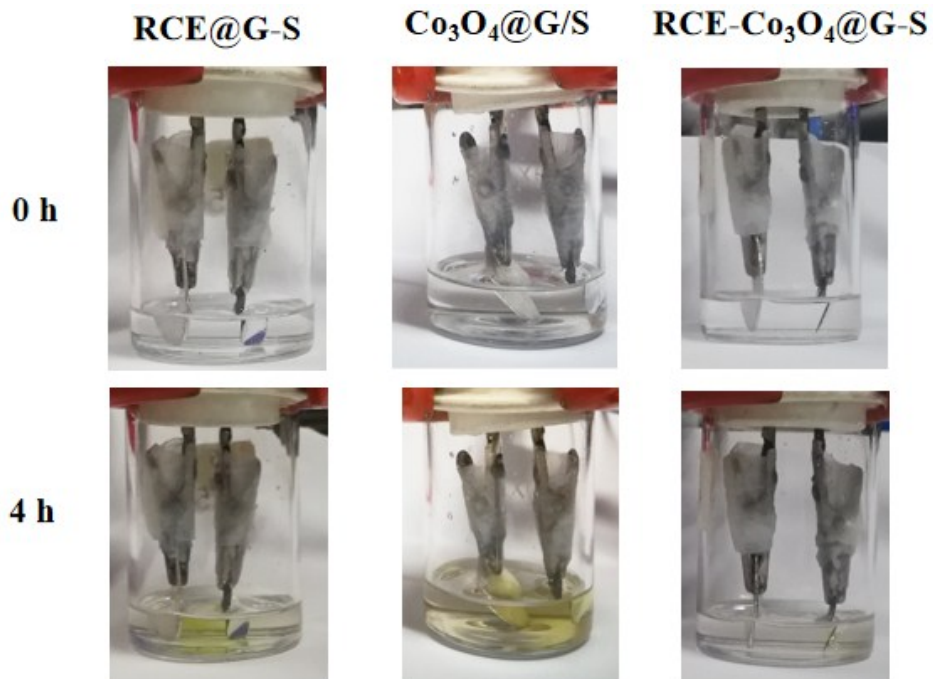

Figure S12. Visual illustration on LiPS confinement effect in cells using RCE@G-S, Co$_3$O$_4$@G-S, and RCE-Co$_3$O$_4$@G-S cathodes respectively.